Nonlinear Dyn (2020) 100:3925–3935
https://doi.org/10.1007/s11071-020-05703-6

ORIGINAL PAPER

Clocking convergence of the fractional difference logistic map

Daiva Petkevičiūtė-Gerlach · Inga Timofejeva · Minvydas Ragulskis

Received: 1 November 2019 / Accepted: 17 May 2020 / Published online: 11 June 2020

Abstract The convergence of the fractional difference logistic map is studied in this paper. A computational technique based on the visualisation of the algebraic complexity of transient processes is employed for that purpose. It is demonstrated that the dynamics of the fractional difference logistic map is similar to the behaviour of the extended invertible logistic map in the neighbourhood of unstable orbits. This counter-intuitive result provides a new insight into the transient processes of the fractional difference logistic map.

Keywords Fractional difference logistic map · Convergence · H-rank · Temporal stabilisation

1 Introduction

The discrete logistic map has been extensively studied since it was presented as one of the first examples of a deterministic system exhibiting chaotic behaviour [23]. Apart from being an interesting research object by itself, the logistic map is attracting attention because of its many possible applications in areas such as population growth modelling, economics [4], cryptography [17, 26], and random number generation [16, 25, 28].

Fractional calculus, although it was already discussed by l'Hospital and Leibniz more than 300 years ago, became a standard technique in the modelling of various real-world systems only in the last few decades [13]. Boosted by the evolution of computers and computational methods, applications of differential equations with fractional derivatives for modelling dynamical systems have expanded to the fields of physics, biology, signal processing, engineering and economics [30]. There is no unique definition of a fractional derivative, and the main alternatives include the definitions of Riemann–Liouville, Grünwald–Letnikov, Riesz [13], and Caputo [5].

As numerical solutions of fractional differential equations require their discretisation, various discretisation schemes have been proposed. Therefore a variety of fractional versions of the discrete logistic map exist, a few of which are obtained only using the Caputo fractional derivative. For example, the fractional logistic map (FLM) was first obtained by Edelman [7, 9] as a special form of the fractional universal map [12]. Wu and Baleanu [32] and later Edelman [10] proposed fractional difference logistic maps (FDLM) as solutions of versions of a fractional

D. Petkevičiūtė-Gerlach
Faculty of Mathematics and Natural Sciences, Kaunas University of Technology, Studentų 50-318, 51368 Kaunas, Lithuania

I. Timofejeva · M. Ragulskis (✉)
Center for Nonlinear Systems, Kaunas University of Technology, Studentų 50-146, 51368 Kaunas, Lithuania
e-mail: minvydas.ragulskis@ktu.lt

difference logistic equation. The difference between the FLM and the FDLM is the use of the power function for the in FLM instead of the falling factorial function (which is asymptotically power function) in FDLM [10].

The main objective of this paper is to explore the convergence of the fractional difference logistic map proposed in [10]. The presentation is structured as follows. Definitions and preliminary results, necessary for the further analysis, are introduced in Sect. 2. Convergence properties of the classical logistic map and the invertible extended logistic map are studied in Sect. 3. Section 4 demonstrates the counterintuitive similarity between the convergence patterns of the invertible extended logistic map and the fractional difference logistic map. The summary of the results and concluding remarks are given in Sect. 5.

2 Preliminaries

2.1 The classical logistic map

The classical logistic map (made famous by May [23]) is a paradigmatic iterative chaotic map. The governing iterative equation of the logistic map reads:

$$x_{k+1} = a\,x_k\,(1 - x_k), \quad k = 0, 1, 2, \ldots, \tag{1}$$

where a is the control parameter (normally assumed as $0 \le a \le 4$) and the initial condition $0 \le x_0 \le 1$.

Note, that the classical logistic map is non-invertible, since (1) cannot be solved for x_k uniquely:

$$x_k = \frac{1}{2} \pm \frac{\sqrt{a^2 - 4\,a\,x_{k+1}}}{2\,a}. \tag{2}$$

2.2 The invertible extended logistic map

A discrete map $x_{k+1} = f(x_k)$ is invertible, if x_k can be computed as

$$x_k = f^{-1}(x_{k+1}), \tag{3}$$

where both f and f^{-1} are single-valued functions.

A one-dimensional non-invertible iterative map can be transformed into an invertible iterative map by increasing its dimension [21]. For example, adding a second equation to the classical logistic map yields the invertible extended logistic map [22]:

$$\begin{cases} x_{k+1} = a\,x_k(1 - x_k) + y_k; \\ y_{k+1} = b\,x_k, \end{cases} \tag{4}$$

where $0 \le a \le 4$, $0 \le b < a$ and $k = 0, 1, 2, \ldots$;

$$\begin{cases} x_k = \dfrac{y_{k+1}}{b}; \\ y_k = x_{k+1} - \dfrac{a}{b^2}\; y_{k+1}(b - y_{k+1}). \end{cases} \tag{5}$$

2.3 The fractional difference logistic map

The fractional difference logistic map studied in this article was introduced in [10] and can be obtained as the integral of the following fractional difference equation:

$$\begin{aligned} {}^{C}\Delta_0^{v} u(t) &= a\,u(t + v - 1)(1 - u(t + v - 1)) \\ &\quad - u(t + v - 1), \\ t \in \mathbb{N}_{d+1-v}, \quad 0 < v \le 1, \quad 0 < a < 4, \quad u(d) &= u_0, \end{aligned} \tag{6}$$

where $\mathbb{N}_d = \{d, d + 1, d + 2, \ldots\}$ with $d \in \mathbb{R}$ fixed, and ${}^{C}\Delta_d^{v}$ is the left Caputo-like delta difference [1], which, for $v > 0$, $m - 1 < v < m$, $m \in \mathbb{N}$ and $t \in \mathbb{N}_{d+m-v}$, is defined as

$${}^{C}\Delta_d^{v} u(t) = \frac{1}{\Gamma(m - v)} \sum_{s=d}^{t-(m-v)} (t - s - 1)^{(m-v-1)} \Delta^m u(s), \tag{7}$$

with a summation index $s \in \mathbb{N}_d$, the falling factorial

$$t^{(v)} = \frac{\Gamma(t + 1)}{\Gamma(t + 1 - v)} \tag{8}$$

and the mth-order forward difference operator

$$\Delta^m u(s) = \sum_{k=0}^{m} \binom{m}{k} (-1)^{m-k}\, u(s + k). \tag{9}$$

If $v = m \in \mathbb{N}$, then [1, 24]

$${}^{C}\Delta_d^{v} u(t) = \Delta^m u(t). \tag{10}$$

Note that, when $m = 1$, as is the case in (6),

$$\Delta^m u(t) = \Delta u(t) = u(t + 1) - u(t). \tag{11}$$

Using the results of [2, 6], for $d = 0$, the discrete integral form of (6) is obtained as

$$u(t) = u_0 + \frac{1}{\Gamma(v)} \sum_{s=1-v}^{t-v} (t-s-1)^{(v-1)} \times (a\,u(s+v-1)\,(1-u(s+v-1)) - u(s+v-1)), \quad t \in \mathbb{N}, \tag{12}$$

and its corresponding numerical formula for $x_k = u(t)$, $k \in \mathbb{N}_0$ can then be presented as

$$x_k = x_0 + \frac{1}{\Gamma(v)} \sum_{j=1}^{k} \frac{\Gamma(k-j+v)}{\Gamma(k-j+1)} \times \left(a\,x_{j-1}\,(1-x_{j-1}) - x_{k-j}\right). \tag{13}$$

Using the property $\Gamma(z+1) = z\,\Gamma(z)$, $z \in \mathbb{Z}$, of the Gamma function, the map (13) can be rewritten in a form, which is more convenient for numerical computations:

$$x_k = x_0 + \sum_{j=1}^{k} G_{j-1}\,\left(a\,x_{k-j}\,(1-x_{k-j}) - x_{k-j}\right). \tag{14}$$

where

$$G_0 = 1, \quad G_j = \left(1 - \frac{1-v}{j}\right) G_{j-1}. \tag{15}$$

By setting the parameter v to 1, (14) gets reduced to the canonical form (1) of the classical logistic map. Another similar fractional map, derived in an analogous way and corresponding to a non-canonical form of the classical logistic map, was proposed in [32] (see also [27]).

In contrast to the classical logistic map (1), the present state x_k in the fractional map (14) depends on all the past states $x_0, x_1, \ldots, x_{k-1}$. In other words, the memory horizon for the fractional difference logistic map is the whole transient process, i.e. (14) is a long-term memory map. Clearly, the fractional difference logistic map is a non-invertible discrete map.

2.4 The algorithm for the estimation of the algebraic complexity of a sequence

Let us consider a sequence of real numbers $(x_k)_{k=0}^{+\infty}$. The Hankel transform of $(x_k)_{k=0}^{+\infty}$ produces a sequence $(h_k)_{k=0}^{+\infty}$, where $h_k = \det(H_k)$ and H_k is a $(k+1)$-order catalecticant Hankel matrix:

$$H_k = \begin{bmatrix} x_0 & x_1 & \ldots & x_k \\ x_1 & x_2 & \ldots & x_{k+1} \\ \vdots & \vdots & \ddots & \vdots \\ x_k & x_{k+1} & \ldots & x_{2k} \end{bmatrix}. \tag{16}$$

If there exists such $m \geq 1$ that $h_m \neq 0$, but $h_j = 0$ for all $j > m$, then $(x_k)_{k=0}^{+\infty}$ is a linear recurrence sequence (LRS) and its order is m [18].

However, all real-world sequences (including sequences generated by iterative maps) are contaminated with noise (due to computational errors or the external noise). Therefore, the order of a real-word sequence is infinite (otherwise it would be possible to reconstruct the mathematical model of noise).

The concept and the computational technique for computing the H-rank of a sequence (even if this sequence is not a LRS) is presented in [19]. The H-rank is defined as the number of squared singular values of the Hankel matrix H_k larger than the machine epsilon [19] (a singular value of H_k is a square root of a nonnegative eigenvalue of $H_k^T H_k$). The H-rank of a sequence is equal to the order of that sequence if and only if this sequence is a LRS [19]. However, it is shown in [19] that the H-rank can serve as a convenient computational tool for the assessment of the algebraic complexity of real-world sequences.

The machine epsilon is set to 10^{-10}, and the dimension of the Hankel matrix H_k is set to 50 in this work. Therefore, if the order of a sequence is greater than 50 or does not exist, the H-rank of that sequence is assigned to 50.

3 Convergence properties of the two classical logistic maps

3.1 Convergence of the classical logistic map

The bifurcation diagram and the plot of H-ranks for the classical logistic map (1) are depicted in Fig. 1.

The bifurcation diagram of the classical logistic map is constructed by setting the initial condition x_0 to 0.5. The transient processes are eliminated by omitting the first 300 steps; 200 steps $(x_{301}, \ldots, x_{500})$ are used to plot the diagram (Fig. 1b).

The plot of H-ranks (Fig. 1a) is constructed without the elimination of the transient processes [20]. The initial condition is not fixed—every point in the plot of

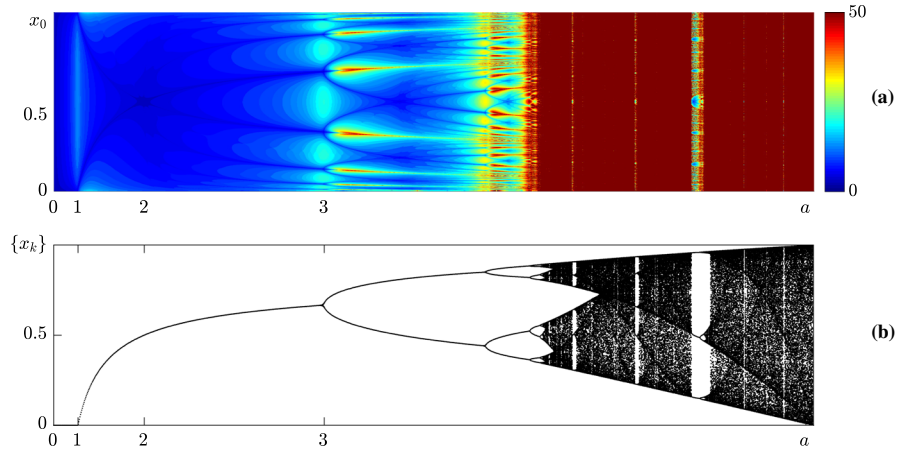

Fig. 1 The plot of H-ranks for the classical logistic map is shown in **a**; each point corresponds to a separate transient process started from the initial condition x_0 and the parameter value a. The bifurcation diagram of the standard logistic map is shown in **b**. Note that the a-axis in both parts is logarithmic for better visualisation

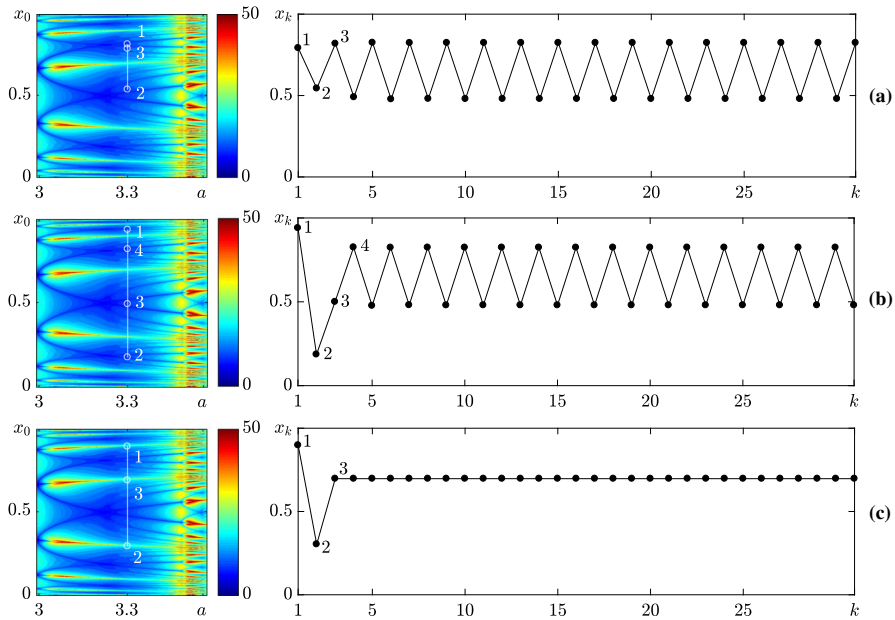

Fig. 2 The classical logistic map can converge in three different ways at $a = 3.3$. Plots on the right column show transient processes started from different initial conditions x_0. Plots on the left column depict the first four discrete points of the transient processes on top of the plots of H-ranks. Asymptotic convergence to the stable period-2 orbit is shown in **a**. Non-asymptotic convergence to the stable period-2 orbit is shown in **b**. Non-asymptotic convergence to the unstable period-1 orbit is shown in **c**

H-ranks corresponds to a separate transient process in the parameter plane (a, x_0), where x_0 varies from 0.01 to 1 by a step of 0.001, and a varies from 0 to 4.

Three different types of transient processes of the classical logistic map (asymptotic convergence to a stable orbit, non-asymptotic convergence to the stable orbit and non-asymptotic convergence to the unstable orbit) are illustrated in Fig. 2 at $a = 3.3$ (at this value of parameter a the period-1 orbit is unstable and the period-2 orbit is stable).

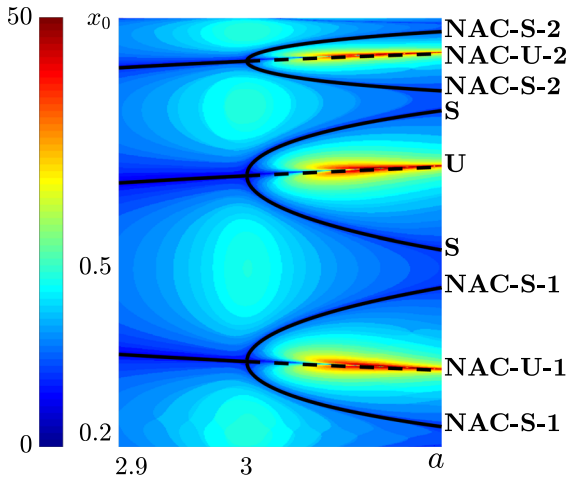

Fig. 3 The plot of H-ranks reveals the NAC manifolds. The symbol U denotes the unstable period-1 orbit (it becomes unstable at $a > 3$). Symbols S denote the stable period-2 orbit. NAC-U denotes the NAC manifold of the unstable period-1 orbit. Numbers at NAC-U show how many time-forward steps are required for reaching the unstable period-1 orbit. Analogously, NAC-S denotes the NAC manifold of the stable period-2 orbit

Figure 2a shows asymptotic convergence to the stable period-2 orbit. The first three points of the transient process are depicted in the left colour plot. Note that the parameter a is constantly fixed to 3.3 during all computational experiments with the classical logistic map.

It is shown in [29] that the plot of H-ranks reveals the manifolds of non-asymptotic convergence (NAC manifolds) for the classical logistic map. Non-asymptotic convergence to the stable period-2 orbit and non-asymptotic convergence to the unstable period-1 orbit is illustrated in Fig. 2b, c. The initial condition is selected on the NAC manifold of the stable period-2 orbit in Fig. 2b and on the NAC manifold of the unstable period-1 orbit in Fig. 2c.

The pattern of H-ranks is zoomed and marked (Fig. 3) in order to clarify the selection of initial conditions in Fig. 2b, c. The symbol U in Fig. 3 denotes the unstable period-1 orbit (the orbit becomes unstable at $a > 3$). Symbols S denote the stable period-2 orbit. NAC-U denotes the NAC manifold of the unstable period-1 orbit. Numbers at NAC-U show how many time-forward steps are required for reaching the unstable period-1 orbit. Analogously, NAC-S denotes the NAC manifold of the stable period-2 orbit. The observation window in Fig. 3 is limited to accommodate only two time-backward steps for clarity.

The initial condition in Fig.2b is selected on NAC-S-2 (Fig. 3). The initial condition $x_0 = 0.9401$ corresponds to a local minimum around the upper dark band of H-ranks (Fig. 3) and results into a non-asymptotic convergence to the stable period-2 orbit in two forward steps (Fig. 2b). Analogously, the initial condition in Fig. 2c is selected on NAC-U-2 (Fig. 3). The value $x_0 = 0.9077$ corresponds to a local maximum around the bright band of H-ranks (Fig. 3) and results into a non-asymptotic convergence to the unstable period-1 orbit in two forward steps (Fig. 2c). All computations in Fig. 2 are performed at $a = 3.3$.

The situation becomes more complex after the second period doubling bifurcation. Then the plot of H-ranks reveals the following intertwined NAC manifolds: the NAC manifold of the unstable period-1 orbit, the NAC manifold of the unstable period-2 orbit, and the NAC manifold of the stable period-4 orbit (Fig. 1a). The situation becomes even more complex as the logistic map goes through the cascade of period doubling bifurcations (Fig. 1a).

3.2 Convergence of the invertible extended logistic map

The convergence of the invertible extended logistic map (4) is completely different from the convergence of the classical logistic map. This is predetermined by the nature of the discrete map—non-asymptotic convergence cannot exist in invertible maps, as shown in [20].

The plot of H-ranks and the bifurcation diagram of the invertible extended logistic map are shown in Fig. 4. Note that only the scalar sequences of $\{x_k\}$; $k = 0, 1, 2, \ldots$ are used to visualise the plot of H-ranks and the bifurcation diagram. The parameter b is fixed to 0.1 and the initial value of y_0 is fixed to 0.01 for all computational experiments with the invertible extended logistic map.

Of course, the plots of H-ranks for the standard logistic map and the invertible extended logistic map are different. However, some similarities between these two plots do exist. The repetitive patterns of red-yellow bands in the plot of H-ranks (for an invertible bouncer system) are denoted as a pseudo-stable structure in [20]. This pseudo-stable structure in Fig. 4a looks similar to the manifold of non-asymptotic convergence (compare to Fig. 1a, which also has a

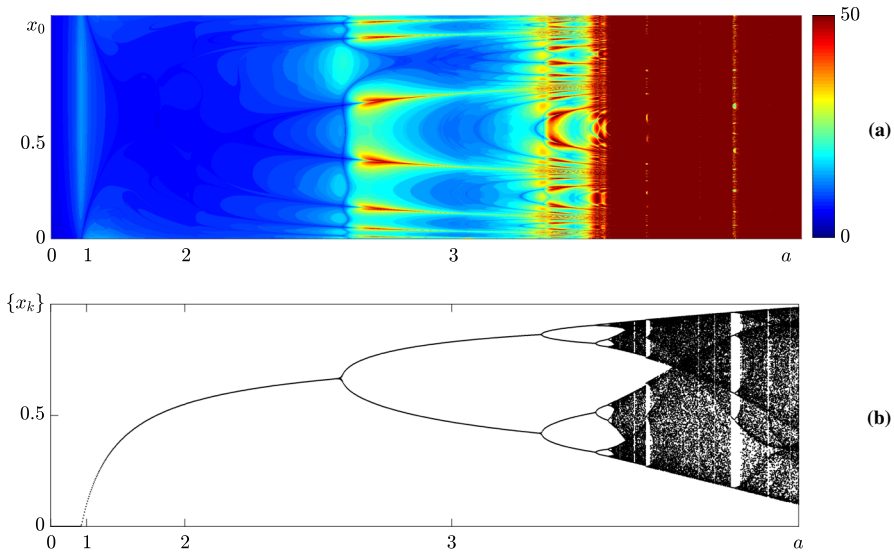

Fig. 4 The plot of H-ranks (**a**) and the bifurcation diagram (**b**) for the invertible extended logistic map. The parameter b is fixed to 0.1; the initial condition y_0 is fixed to 0.01. The scale of the a-axis in both parts is logarithmic for the clarity of presentation

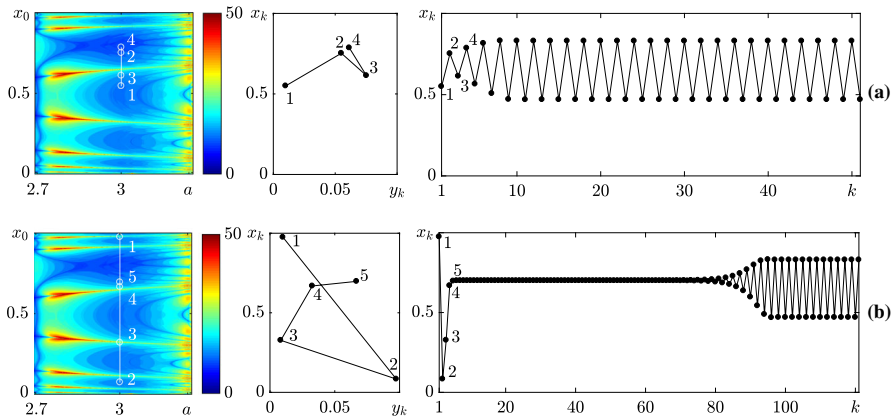

Fig. 5 Asymptotic convergence of the sequence $\{x_k\}$, $k = 0, 1, 2, \ldots$ to the stable period-2 orbit of the invertible extended logistic map at $a = 3$; $b = 0.1$; $y_0 = 0.01$. Plots on the right column show the x_k values of the two-dimensional transient processes started from different initial conditions x_0, with the first few points numbered. The middle column shows the same numbered points in the y–x plane: a trajectory started from the point 2 will only go to point 3, if both coordinates, x_2 and y_2, will be used as the initial point. Plots on the left column depict the first x_k values of the transient processes on top of the plots of H-ranks of the sequence $\{x_k\}$. The transient process converging directly to the stable period-2 orbit is shown in **a**. Temporary stabilisation of the unstable period-1 orbit and subsequent asymptotic convergence to the stable period-2 orbit is shown in **b**. **b** Illustrates the fact that a non-asymptotic convergence does not exist in invertible maps

repetitive pattern of red-yellow bands)—but such convergence cannot exist in the invertible extended logistic map!

It appears that the pseudo-stable structure of bands in the H-rank plot in Fig. 4a does represent the manifold of initial conditions which can be used to temporarily stabilise unstable orbits [20]. Computational illustrations in Fig. 5 are used to visualise this nonlinear effect in the invertible extended logistic map at $a = 3$ (b and y_0 remain fixed to 0.1 and 0.01 accordingly).

A stable period-2 orbit and an unstable period-1 orbit do exist in the invertible extended logistic map at $a = 3$ and $b = 0.1$ [22]. Asymptotic convergence to the stable period-2 orbit is illustrated in Fig. 5a. The convergence rate to the stable period-2 orbit can be higher or lower—that is represented by different colours in the plot of H-ranks. However, in contrast to the classical logistic map, the convergence to the stable period-2 orbit cannot be non-asymptotic.

The nature of the pseudo-stable structure in Fig. 4a is illustrated in Fig. 5b. The initial condition x_0 is set exactly on one of the bands in the plot of H-ranks (Fig. 5b; y_0 remains fixed to 0.01). It seems like the system is trying to converge non-asymptotically to the unstable period-1 orbit (Fig. 5b). However, non-asymptotic convergence is forbidden in invertible maps. Sooner or later the transient process converges asymptotically to the stable period-2 orbit (Fig. 5b). Such an effect is named as temporary stabilisation of unstable orbits in invertible maps [20].

Note that analytical techniques cannot be used to identify the bands in the plot of H-ranks for the invertible extended logistic map. This is a purely computational exercise—which is in a stark contrast to the classical logistic map where the centres of the bands in the plot of H-ranks can be simply determined by backward iterations from the unstable orbits [29].

4 Convergence of the fractional difference logistic map

The fixed points of fractional difference logistic map (14) for all v are the same as those of the classical logistic map: $x = 0$ and $x = \frac{a-1}{a}$. The bifurcation diagram is also independent of x_0, as long as x_0 is not a fixed point (though the memory horizon of any transient trajectory reaches x_0). However, as shown in [8] for Caputo standard maps, the whole diagram can shift right or left along the a axis depending on the number of values skipped at the beginning of the sequence for plotting the diagram. The same procedure as described in Sect. 3.2 is used for plotting the bifurcation diagram of the fractional difference logistic map.

Such a diagram for $v = 0.8$ is shown in Fig. 6b. It appears that for smaller values of a, the transient processes generated by the fractional difference logistic map converge to the fixed point $x = \frac{a-1}{a}$. Then, after the first period doubling bifurcation at $a \approx 2.7$, a period-2 orbit is born. The second period doubling bifurcation occurs at $a \approx 3.3$. Further increase in a yields a cascade of period-doubling bifurcations resulting into chaotic orbits (Fig. 6b).

The map of H-ranks for the fractional difference logistic map is shown in Fig. 6a. The values of a are varied from 0 to 3.8; the initial condition x_0 – from 0 to 1 and v is fixed to 0.8. The transient sequences $\{x_k\}$, $k = 0, 1, \ldots, 100$ are constructed for each pair of (a, x_0). The upper limit of the rank of the sequence (set to 50) blocks the region of the parameter plane where the transient processes become chaotic (Fig. 6a). However, a repetitive pattern of red-yellow bands in the H-ranks plot is visible right after the first period doubling bifurcation (Fig. 6a).

In order to explore this pattern of H-ranks we set a to 3 (v remains fixed to 0.8) and plot transient processes from different initial conditions (Fig. 7). As there are only two (unstable) fixed points, any trajectory, that is not a fixed point, is approaching the stable asymptotically period-2 orbit at $a = 3$. Note that only asymptotically periodic solutions (if period is greater than one) exist in fractional and fractional difference systems [3, 14, 15, 31, 33].

Clearly, one should not expect the existence of non-asymptotic convergence to the period-2 orbit (around $a = 3$). Computational experiments (Figs. 7, 8) show that transient processes started from the centres of the pattern-forming bands in the plot of H-ranks (at $a = 3$ in Fig. 6) approach the unstable period-1 orbit in a few time forward steps. Then these transient processes gradually evolve into a period-2 orbit (Fig. 8). As mentioned previously, this is not a non-asymptotic convergence to an unstable period-1 orbit. Trajectories, when a bifurcation or a cascade of bifurcations occurs not as a result of a change in a system's parameter, but on a single attracting trajectory during its time evolution, were noticed and explored in fractional maps before [7]. However, this process strikingly reminds the transient process exhibited by the inverted extended logistic map (Fig. 5b). That is a completely unexpected result.

Another astonishing fact is that the number of bands in Fig. 6a at $a = 3$ is countable but infinite. From the first glance, this seems a natural feature—the intersection of the stable and the unstable manifolds in the

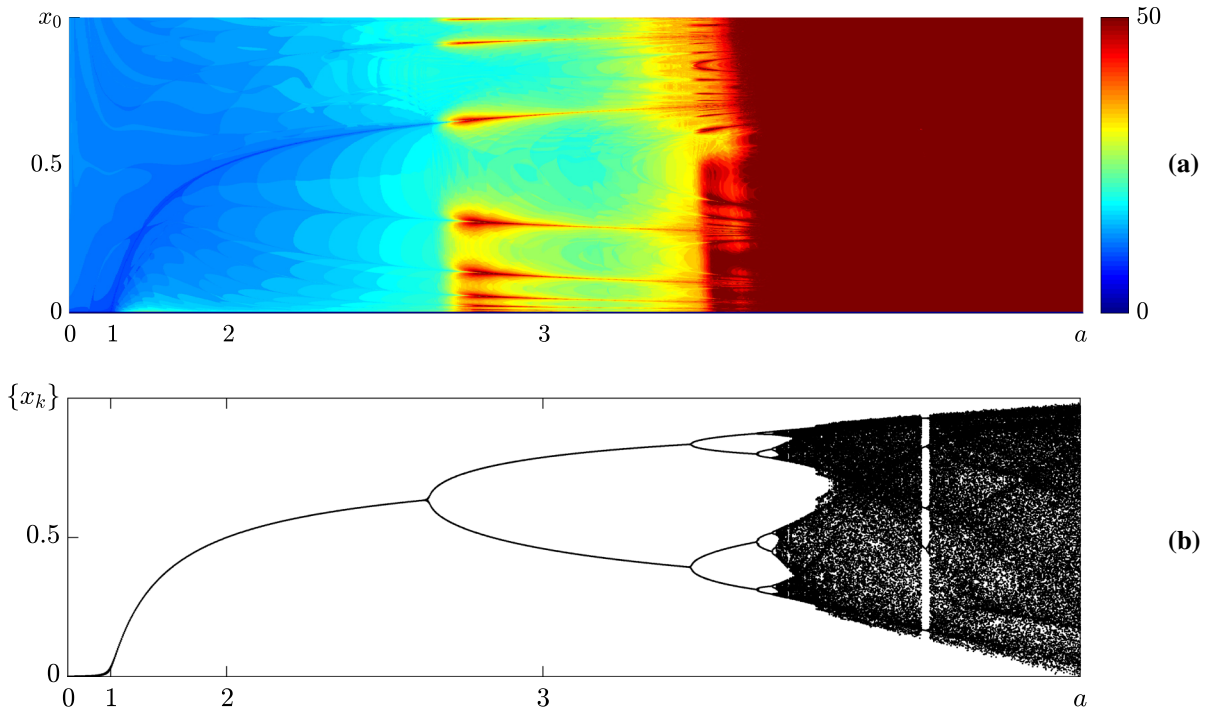

Fig. 6 The plot of H-ranks (**a**) and the bifurcation diagram (**b**) of the fractional difference logistic map at $v = 0.8$. The scale of the a axis is chosen to be logarithmic in both parts for clarity. The maximum rank of a transient sequence is set to 50

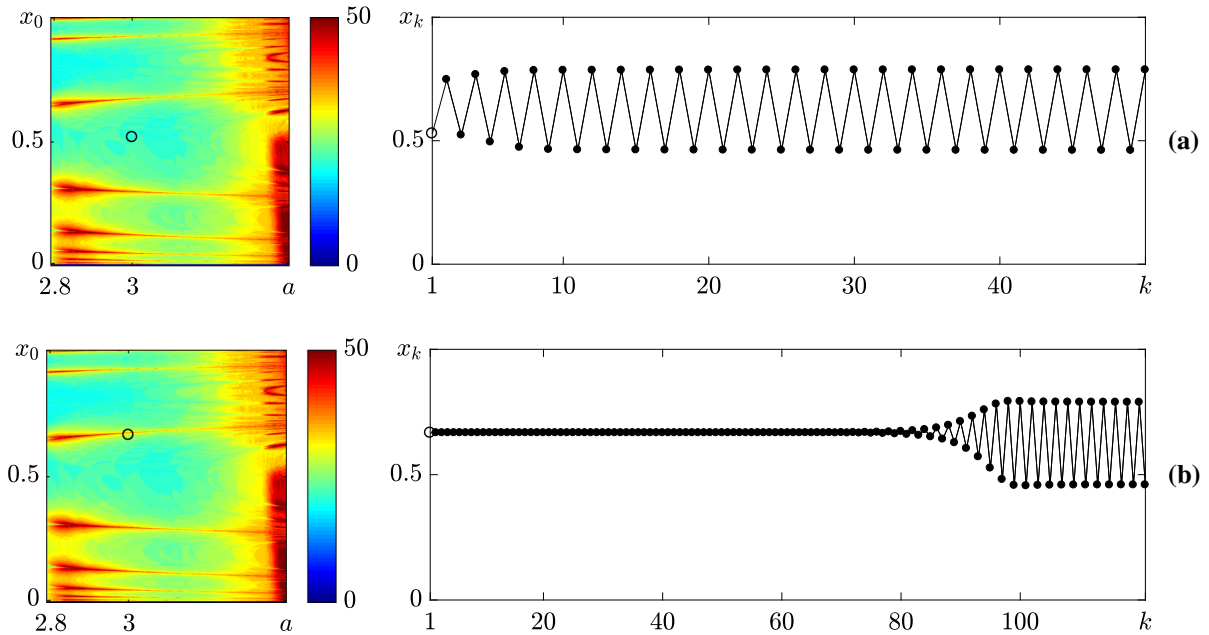

Fig. 7 Convergence of the fractional difference logistic map at $a = 3$ and $v = 0.8$. Asymptotic convergence to the stable asymptotically period-2 orbit is shown in **a**. Temporary stabilisation of the unstable period-1 orbit and eventual asymptotic convergence to the period-2 orbit is shown in **b**. Initial conditions are marked on the plots of H-ranks in the left columns of **a** and **b**

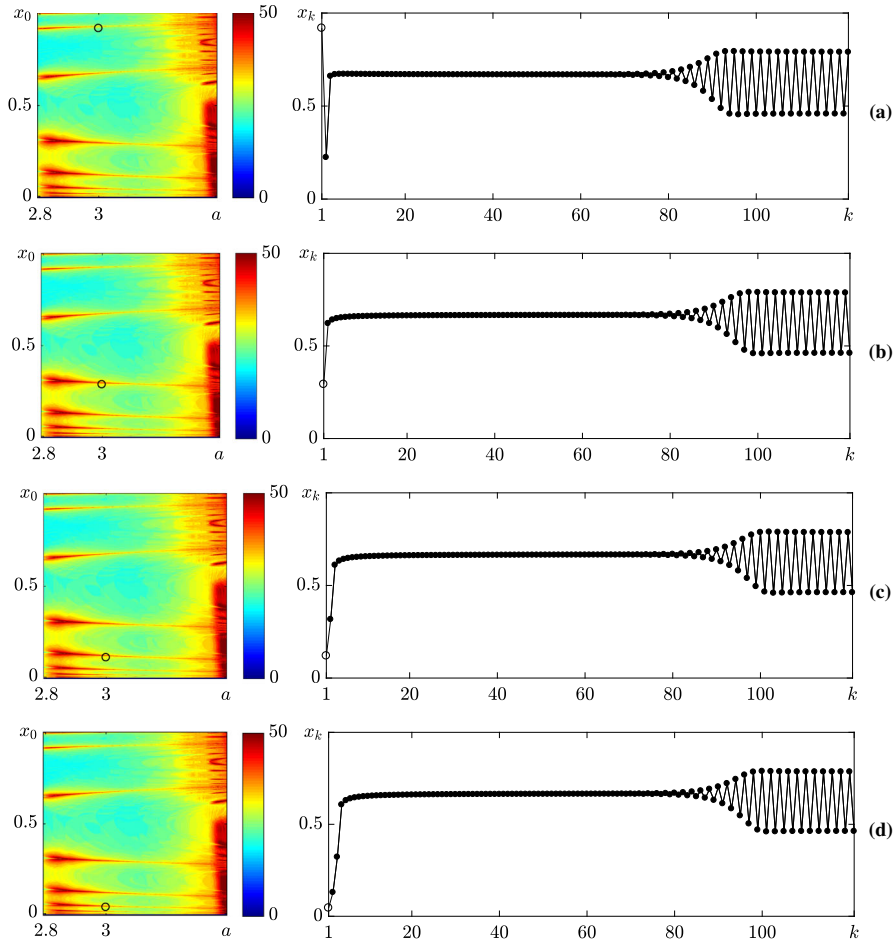

Fig. 8 Temporary stabilisation of the unstable period-1 orbit in the fractional difference logistic map at $a = 3$ and $v = 0.8$. Initial conditions in **a–d** are selected on the consecutive bands in the plot of H-ranks

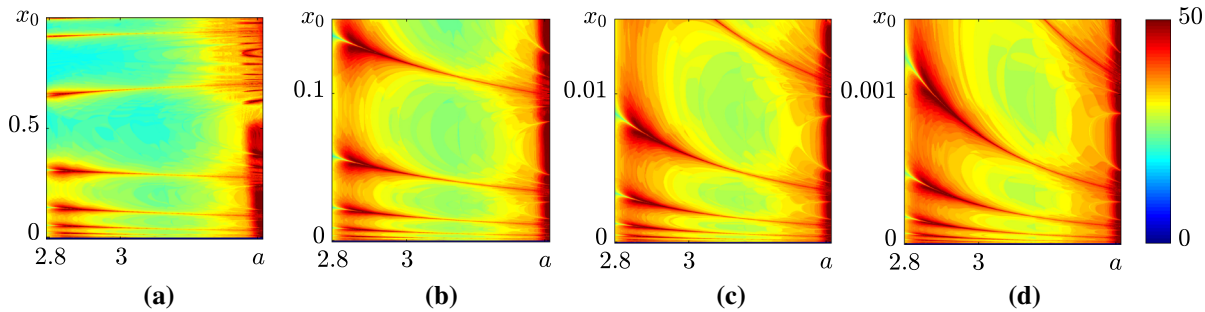

Fig. 9 The number of bands in the plot of H-ranks for the fractional difference logistic map is countable but infinite. Parameter v is set to 0.8; parameter a is varied in the interval [2.8, 3.3]. Note that the range of the vertical axis is zoomed in **a–d**

classical logistic map gives rise to an infinite manifold of non-asymptotic convergence [20]. However, the structure of the fractional difference logistic map is completely different from the classical logistic map. Nevertheless, Fig. 9 provides a computational evidence that the number of bands (and the number of initial conditions temporary stabilising the unstable period-1 orbit) is infinite.

5 Conclusions

The convergence of the fractional difference logistic map is explored in this paper. It is demonstrated that the fractional difference logistic map possesses interesting and counterintuitive features. In agreement with [7], it is shown that memory effects in fractional discrete systems do not eliminate the possibility of the temporary stabilisation of unstable orbits (cascade of bifurcations type trajectories). Algorithms capable to determine the algebraic complexity of transient processes are used to construct the plot of H-ranks for the fractional difference logistic map.

This ability to temporarily stabilise unstable orbits in discrete maps with memory effects opens a new range of possible applications. One of the potential applications could be in the area of digital information coding and communication. An unstable orbit (not necessarily the period-1 orbit) could be temporarily stabilised—and an eavesdropper could be fooled about the communication protocol. Then, the transient process will evolve to a higher period orbit—and the communication process could be started after a certain delay in time. The parameters of the communication algorithm do not need to be changed in the process.

Another possible application of the presented results is an effective determination of initial conditions leading to CBTT trajectories, which have already been used for modelling of lifespans of living species [11]. These applications remain as possible objectives for future studies.

Compliance with ethical standards

Conflict of interest The authors declare that they have no conflict of interest.

References

1. Abdeljawad, T.: On Riemann and Caputo fractional differences. Comput. Math. Appl. **62**, 1602–1611 (2011)
2. Anastassiou, G.A.: Discrete fractional calculus and inequalities. arXiv e-prints arXiv:0911.3370 (2009)
3. Area, I., Losada, J., Nieto, J.J.: On fractional derivatives and primitives of periodic functions. Abstr. Appl. Anal. **2014**, 392598 (2014)
4. Ausloos, M., Dirickx, M.: The Logistic Map and the Route to Chaos: From the Beginnings to Modern Applications. Springer, Berlin (2006)
5. Caputo, M.: Linear models of dissipation whose Q is almost frequency independent-II. Geophys. J. Int **13**(5), 529–539 (1967)
6. Chen, F., Luo, X., Zhou, Y.: Existence results for nonlinear fractional difference equation. Adv. Differ. Equ. **2011**(1), 1–12 (2010)
7. Edelman, M.: Universal fractional maps and cascade of bifurcations type attractors. Chaos **23**, 033127 (2013)
8. Edelman, M.: Caputo standard α-family of maps: fractional difference vs. fractional. Chaos **24**, 023137 (2014)
9. Edelman, M.: Fractional maps as maps with power-law memory. In: Afraimovich, V., et al. (eds.) Nonlinear Dynamics and Complexity, Nonlinear Systems and Complexity, vol. 8, pp. 79–120. Springer, New York (2014)
10. Edelman, M.: Fractional maps and fractional attractors. Part II: fractional difference Caputo α-families of maps. Interdiscip. J. Discontin. Nonlinearity Complex. **4**, 391–402 (2015)
11. Edelman, M.: Evolution of systems with power-law memory: do we have to die? arXiv e-prints arXiv:1904.13370 (2019)
12. Edelman, M., Tarasov, V.: Fractional standard map. Phys. Lett. A **374**, 279 (2009)
13. Hilfer, R.: Applications of Fractional Calculus in Physics. World Scientific Publishing, Singapore (2000)
14. Jonnalagadda, J.M.: Periodic solutions of fractional nabla difference equations. Commun. Appl. Anal. **20**, 585–609 (2016)
15. Jonnalagadda, J.M.: Quasi-periodic solutions of fractional nabla difference systems. Fract. Differ. Calc. **7**(2), 339–355 (2017)
16. Kanso, A., Smaoui, N.: Logistic chaotic maps for binary numbers generations. Chaos Solitons Fractals **40**(5), 2557–2568 (2009)
17. Kocarev, L., Jakimoski, G.: Logistic map as a block encryption algorithm. Phys. Lett. A **289**(4), 199–206 (2001)
18. Kurakin, A., Kuzmin, A., Nechavev, A.: Linear complexity of polinear sequences. J. Math. Sci. **76**, 2793–2915 (1995)
19. Landauskas, M., Navickas, Z., Vainoras, A., Ragulskis, M.: Weighted moving averaging revisited: an algebraic approach. Comput. Appl. Math. **36**, 1545–1558 (2017)
20. Landauskas, M., Ragulskis, M.: A pseudo-stable structure in a completely invertible bouncer system. Nonlinear Dyn. **78**, 1629–1643 (2014)
21. López-Ruiz, R., Fournier-Prunaret, D., Nishio, Y., Grácio, C.: Nonlinear Maps and Their Applications: Selected Contributions from the NOMA 2013 International Workshop. Springer Proceedings in Mathematics & Statistics. Springer, Berlin (2015)
22. Lu, G., Landauskas, M., Ragulskis, M.: Control of divergence in an extended invertible logistic map. Int. J. Bifurc. Chaos **28**(10), 1850129 (2018)
23. May, M.R.: Simple mathematical models with very complicated dynamics. Nature **261**, 459–467 (1976)
24. Miller, K.S., Ross, B.: Fractional difference calculus. In: Srivastava, H.M., Owa, S. (eds.) Univalent Functions, Fractional Calculus, and Their Applications, pp. 139–151. Ellis Horwood, Chichester (1989)
25. Murillo-Escobar, M.A., Cruz-Hernández, C., Cardoza-Avendaño, L., Méndez-Ramírez, R.: A novel

pseudorandom number generator based on pseudorandomly enhanced logistic map. Nonlinear Dyn. **87**(1), 407–425 (2017)
26. Pareek, N., Patidar, V., Sud, K.: Image encryption using chaotic logistic map. Image Vis. Comput. **24**(9), 926–934 (2006)
27. Peng, Y., Sun, K., He, S., Wang, L.: Comments on "Discrete fractional logistic map and its chaos" [Nonlinear Dyn. 75, 283–287 (2014)]. Nonlinear Dyn. **97**(1), 897–901 (2019)
28. Phatak, S.C., Rao, S.S.: Logistic map: a possible random-number generator. Phys. Rev. E **51**, 3670–3678 (1995)
29. Ragulskis, M., Navickas, Z.: The rank of a sequence as an indicator of chaos in discrete nonlinear dynamical systems. Commun. Nonlinear Sci. Numer. Simul. **16**, 2894–2906 (2011)
30. Sun, H., Zhang, Y., Baleanu, D., Chen, W., Chen, Y.: A new collection of real world applications of fractional calculus in science and engineering. Commun. Nonlinear Sci. Numer. Simul. **64**, 213–231 (2018)
31. Tavazoei, M.S., Haeri, M.: A proof for non existence of periodic solutions in time invariant fractional order systems. Automatica **45**, 1886–1890 (2009)
32. Wu, G.C., Baleanu, D.: Discrete fractional logistic map and its chaos. Nonlinear Dyn. **75**, 283–287 (2014)
33. Yazdani, M., Salarieh, H.: On the existence of periodic solutions in time-invariant fractional order systems. Automatica **47**, 1834–1837 (2011)